Proceedings of the 7th GACM Colloquium on Computational Mechanics
for Young Scientists from Academia and Industry
October 11-13, 2017 in Stuttgart, Germany

A 3D peridynamic model of rock cutting with TBM disc cutters

Sahir Butt[1]* and Günther Meschke[1]

Micro Abstract

This study presents computational simulation of rock cutting process using disc cutters, a typical process involved in mechanized rock excavation works. Peridynamics, a nonlocal continuum formulation, is used to model the LCM (linear cutting machine) test of rock cutting with a single TBM (tunnel boring machine) disc cutter. The presented numerical model enables the investigation of different cutting forces as well as of the stress and pressure distribution during the tool-rock interaction.

[1]Institute for Structural Mechanics, Ruhr University Bochum, Germany
***Corresponding author**: sahir.butt@rub.de

Introduction

In an excavation process using a Tunnel Boring Machine (TBM), rock cutting is performed by means of cutting discs (see Fig.1b) installed on a rotating cutter head (see Fig.1a) of the TBM, which is pressed against the tunnel face. As the disc is forced into the rock, a crushed zone develops. As the disc continues to move further, the stresses are further increased in the crushed zone and radial cracks are initiated, as shown in Fig.1c. These cracks coalesce with the cracks initiated from the adjacent cutting disc and the rock mass is disintegrated. This interaction between the rock and a cutting disc can be characterized by the reaction force at the disc. The reaction force is decomposed into normal, rolling and side forces, depicted in Fig.1d. These forces for a single disc cutter needs to be estimated in order to predict the performance of a TBM, i.e. the global torque and thrust requirements. A Linear Cutting Machine (LCM) test [5] was developed at the Colorado School of Mines (CSM), which it is used to predict the performance of a single cutting tool. In the LCM experiment the cutting disc moves along the rock specimen at a known penetration level and the cutting forces (see Fig.1d) are measured at the cutting disc.

A number of empirical models have been developed for the estimation of the process parameters (such as required thrust, penetration rate, specific energy, etc.). One of the popular performance prediction models in this category is the Colorado School of Mines (CSM) model [5]. However, empirical models are restricted by the availability of historical data as well as details of the rock material properties. Alternatively, numerical analysis can be applied to simulate the LCM test, which can incorporate a larger range of rock material properties as compared to empirical models. The excavation process in brittle rock involves complex fracture paths and fragmentation. In this study, we model this process using peridynamics [1, 6, 7], a recently developed nonlocal continuum model, which provides a suitable environment to model physical phenomena involving discontinuities. Simulations of LCM test are carried out at different level of penetrations and the cutting forces are compared with the experimental results presented in [2].

Peridynamic formulation

The peridynamic continuum formulation allows the direct interaction of a material point $\mathbf{x}$ with a set of material points $\mathbf{x}'$, within a volume defined by a cut-off radius δ, known as the peridynamic horizon $\mathscr{H}_x$ [6]. This notion of direct connectivity between the material points is referred to as a *bond*. For a three dimensional peridynamic body, the balance of momentum at a material point $\mathbf{x}$, at time t, is given by

$$\rho(\mathbf{x},t)\frac{\partial^2 \mathbf{u}(\mathbf{x},t)}{\partial t^2} = \int_{\mathscr{H}_x} \left[\underline{\mathbf{T}}[\mathbf{x},t]\langle \mathbf{x}'-\mathbf{x}\rangle - \underline{\mathbf{T}}[\mathbf{x}',t]\langle \mathbf{x}-\mathbf{x}'\rangle \right] dV_{\mathbf{x}'} + \mathbf{b}(\mathbf{x},t), \qquad (1)$$
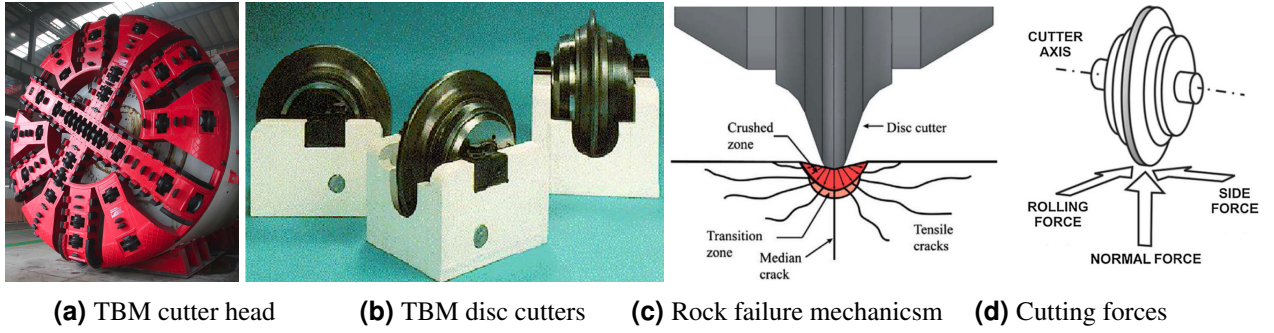
(a) TBM cutter head   **(b)** TBM disc cutters   **(c)** Rock failure mechanicsm   **(d)** Cutting forces

Figure 1. Illustration of disc cutters in TBMs

where $\underline{\mathbf{T}}[\mathbf{x}, t]$ is the *force state* at $\mathbf{x}$ and $\underline{\mathbf{T}}[\mathbf{x}, t]\langle \mathbf{x}' - \mathbf{x}\rangle$ is the force, which a material point $\mathbf{x}$ exerts on $\mathbf{x}'$. Angular brackets are used to denote quantities that $\underline{\mathbf{T}}$ operates on. For an ordinary state-based peridynamic model [7], the force state $\underline{\mathbf{T}}[\mathbf{x}, t]$ is characterized by a magnitude, i.e. a scalar state $\underline{t}[\mathbf{x}, t]$ and a direction, provided by the unit vector state $\underline{\mathbf{M}}[\mathbf{x}, t]$:

$$\underline{\mathbf{T}}[\mathbf{x}, t] = \underline{t}[\mathbf{x}, t]\,\underline{\mathbf{M}}[\mathbf{x}, t], \qquad \underline{\mathbf{M}}[\mathbf{x}, t]\langle \boldsymbol{\xi}\rangle = \frac{\underline{\mathbf{Y}}[\mathbf{x}, t]\langle \boldsymbol{\xi}\rangle}{|\underline{\mathbf{Y}}[\mathbf{x}, t]\langle \boldsymbol{\xi}\rangle|} = \frac{\mathbf{y}' - \mathbf{y}}{|\mathbf{y}' - \mathbf{y}|}, \tag{2}$$

$\underline{\mathbf{Y}}[\mathbf{x}, t]$ is the *deformation state* defined as $\underline{\mathbf{Y}}[\mathbf{x}, t]\langle \mathbf{x}' - \mathbf{x}\rangle = \mathbf{y}' - \mathbf{y} = (\mathbf{x}' + \mathbf{u}') - (\mathbf{x} + \mathbf{u})$, where $\mathbf{y}' - \mathbf{y}$ and $\mathbf{u}' - \mathbf{u}$ are the deformed relative position vector and the relative displacement vector of the bond $\mathbf{x}' - \mathbf{x}$ (see Fig.2a). The scalar force state $\underline{t}[\mathbf{x}, t]$ depends on a scalar stretch-like quantity, denoted as the extension state $\underline{e}[\mathbf{x}, t]$ which characterizes the kinematics of the model, it is defined as $\underline{e}\langle \boldsymbol{\xi}\rangle = |\underline{\mathbf{Y}}\langle \boldsymbol{\xi}\rangle| - |\boldsymbol{\xi}|$, where we use $\mathbf{x}' - \mathbf{x} = \boldsymbol{\xi}$. The extension state $\underline{e}$ is further decomposed additively into an isotropic ($\underline{e}^i$) and a deviatoric ($\underline{e}^d$) extension states. The isotropic extension state is then represented in terms of a scalar-valued volume dilatation $\theta(\underline{e})$ that is defined to match the volumetric strain of a classical continuum model under isotropic loading conditions.

(a) Kinematics of a peridynamic body: undeformed (left) and deformed (right)   **(b)** Scematic of missing peridynamic bonds [4]
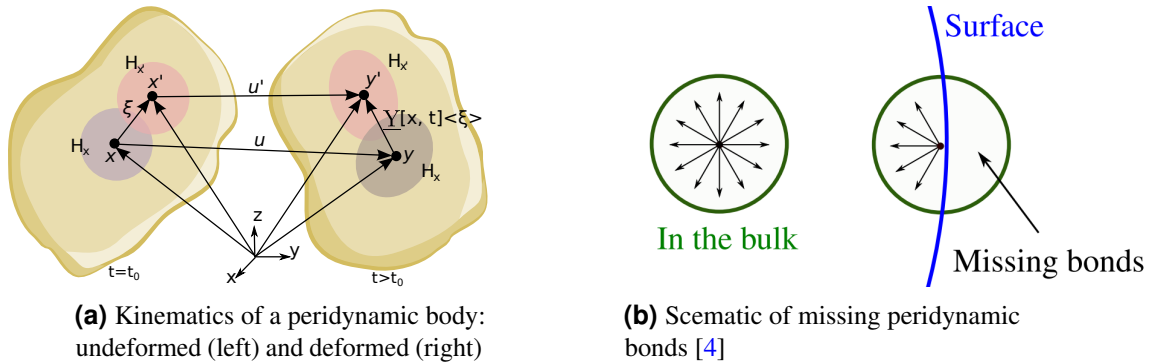
Figure 2

Damage in peridynamics is modeled by breaking the connection/bond between particles. A bond is not allowed to contribute in the internal force calculation once it is broken. In this study we use a critical stretch criteria to break the bonds. The bond between two particles breaks irreversibly once the stretch ($s = \underline{e}\langle \boldsymbol{\xi}\rangle / |\boldsymbol{\xi}|$) exceeds the predefined critical stretch s_c. The critical stretch is calibrated by performing a series of tensile tests and the stretch which reproduces the tensile strength of the material is selected.

PALS model

Due to the nonlocal nature of peridynamics, it becomes inaccurate at points near the surface because some of the peridyamic bonds that would be present in the interior of the material are missing as shown in Fig.2b. In the PALS model, to compute the elastic energy density at a point, two different influence functions (the functions giving weights to nonlocal integrals) are used for the isotropic and the deviatoric deformations. According to [4], it is defined as

$$W(\theta, \underline{e}^d) = \frac{1}{2}K\theta^2 + \mu(\underline{\sigma}\,\underline{e}^d) \bullet \underline{e}^d, \qquad \theta = (\underline{\omega}\,\underline{x}) \bullet \underline{e}, \tag{3}$$

where, $\underline{x}$ is a scalar state with $\underline{x}\langle\boldsymbol{\xi}\rangle = |\boldsymbol{\xi}|$, $\underline{\omega}$ is the dilatation influence function, $\underline{\sigma}$ is the deviatoric influence function and the symbol '•' denotes the dot product of two states as defined in [7].

The influence function $\underline{\omega}$ is found by starting from an initial influence function $\underline{\omega}_0$, which is arbitrary. Furthermore, k linearly independent deformation gradient tensors $\mathbf{H}^k$ are chosen (In three dimensions, $k = 6$ is sufficient because there can be only six linearly independent strain tensors). The extension state $\underline{e}^k$ corresponding to the deformation gradient $\mathbf{H}^k$ is found as $\underline{e}^k\langle\boldsymbol{\xi}\rangle = (\boldsymbol{\xi} \cdot \mathbf{H}^k \cdot \boldsymbol{\xi})/|\boldsymbol{\xi}|$. Now the influence function $\underline{\omega}$ is constructed as an approximation of $\underline{\omega}_0$, satisfying the constraint that the dilatation evaluated using Eq.(3)$_2$ with the extension state $\underline{e}^k$ equals the trace of the deformation gradient $\mathbf{H}^k$. To find $\underline{\omega}$, a functional I is defined as

$$I(\underline{\omega}, \lambda^1, \ldots, \lambda^k) = \frac{1}{2}(\underline{\omega} - \underline{\omega}_0) \bullet (\underline{\omega} - \underline{\omega}_0) - \sum_{i=1}^{k} \lambda^i[(\underline{\omega}\,\underline{x}) \bullet \underline{e}^i - trace(\mathbf{H}^i)]. \tag{4}$$

The functional I is required to be stationary with respect to $\underline{\omega}$ and $\lambda^1, \ldots, \lambda^k$, leading to

$$\frac{\partial I}{\partial \underline{\omega}} = 0 \implies \underline{\omega} = \underline{\omega}_0 + \sum_{j=1}^{k} \lambda^j \underline{x}\,\underline{e}^j, \quad \frac{\partial I}{\partial \lambda^k} = 0 \implies (\underline{\omega}\,\underline{x}) \bullet \underline{e}^k = trace(\mathbf{H}^k). \tag{5}$$

To evaluate $\lambda^1, \ldots, \lambda^k$, we solve a $k \times k$ system of equations given by Eq.(5)$_2$. Once $\lambda^1, \ldots, \lambda^k$ are known, the influence function $\underline{\omega}$ is constructed according to Eq.(5)$_1$ and normalized with a constant factor c, to satisfy $(c\,\underline{\omega}\,\underline{x}) \bullet \underline{x} = D$, where D is the number of dimensions. A similar procedure is followed for the deviatoric influence function $\underline{\sigma}$ (see [4] for details).

Contact formulation

The most common method used to model contact in peridynamics is the *short-range force* approach of Silling and Askari [6]. The normal and tangential contact forces are exerted at a peridynamic node $\mathbf{y}$ by all the nodes $\mathbf{y}_j$ in a close proximity satisfying $|\mathbf{y}_j - \mathbf{y}| < r_c$, where r_c is a predefined contact radius. The normal contact force $\mathbf{f}_n(\mathbf{y}_j - \mathbf{y})$ (i.e. the force that $\mathbf{y}_j$ exerts on $\mathbf{y}$) is found using

$$\mathbf{f}_n(\mathbf{y}_j - \mathbf{y}) = c_f \left(\frac{|\mathbf{y}_j - \mathbf{y}| - r_c}{\delta} \right) V_j\, \mathbf{n}_n, \quad \mathbf{n}_n = \frac{(\mathbf{y}_j - \mathbf{y})}{|\mathbf{y}_j - \mathbf{y}|}. \tag{6}$$

V_j is the volume of the node $\mathbf{y}_j$ and c_f is a constant coefficient representing the stiffness for the repulsive forces [3]. Tangential/frictional force $\mathbf{f}_t$ is calculated using the normal force $\mathbf{f}_n$ as

$$\mathbf{f}_t(\mathbf{y}_j - \mathbf{y}) = -\mu\,|\mathbf{f}_n(\mathbf{y}_j - \mathbf{y})|\,\mathbf{n}_t, \quad \mathbf{n}_t = \frac{\mathbf{v}_{rel}}{|\mathbf{v}_{rel}|}. \tag{7}$$

μ is the coefficient of friction and $\mathbf{n}_t$ is a unit vector in the direction of the relative tangential velocity $\mathbf{v}_{rel}$ of the nodes $\mathbf{y}$ ad $\mathbf{y}_j$. Finally, the total contact force $\mathbf{f}_c$ at the node $\mathbf{y}$ is found by the sum of $\mathbf{f}_n(\mathbf{y}_j - \mathbf{y})$ and $\mathbf{f}_t(\mathbf{y}_j - \mathbf{y})$, from Eq.(6) and Eq.(7) for all $\mathbf{y}_j$ nodes.

Numerical analysis of the LCM test

Numerical simulations of the LCM test are carried out with a single disc cutter of $0.4318m$ diameter. The rock specimen with the dimensions of $0.4m \times 0.4m \times 0.15m$ is used in the simulation. The experiment [2] was carried out with a Colorado red granite sample at different level of penetrations at three different spacings. The penetration p is kept at a constant value for each cut. The material parameters for the rock specimen are used as in the experiment from [2]. By calibration, the critical stretch $s_c = 0.0022m$ is found to reproduce the tensile strength of the rock used in the experiment. The domain is discretized with a resolution of $0.005m$ and the peridynamic horizon is selected as $\delta = 0.016m$. Simulations are carried out using *Peridigm* [3], a peridynamics code developed at Sandia National Laboratories. In Fig.3a, simulation of the LCM test with a single disc cutter, at a penetration of $p = 7mm$ is shown. The average normal forces obtained from peridynamic simulations are plotted against different levels of penetration ($p = 3, 4, 6, 7mm$) in Fig.3b, they show a good agreement with the experimental data [2] (with a disc spacing of $76mm$).
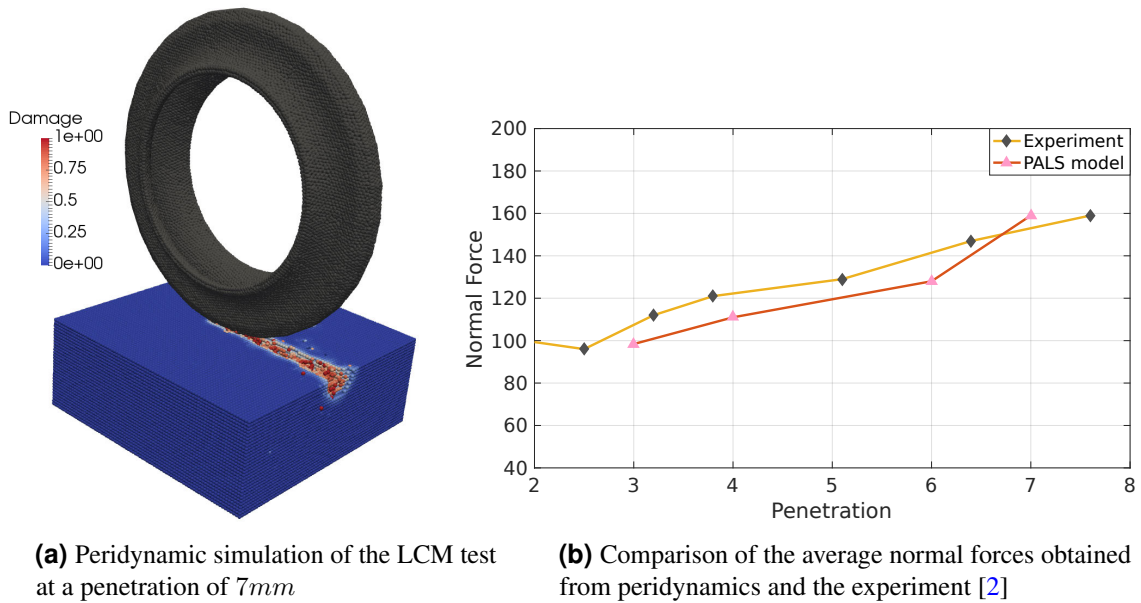
(a) Peridynamic simulation of the LCM test at a penetration of $7mm$

(b) Comparison of the average normal forces obtained from peridynamics and the experiment [2]

Figure 3

Conclusions

A peridynamic model for rock cutting using disc cutters is presented. To address the surface effects of peridynamics, a Position Aware Linear Solid (PALS) material model is used. A number of simulations for the LCM test at different level of penetrations are carried out. The average normal cutting force computed from peridynamics is compared with the experimental data for different level of penetrations. The simulation results are in a good agreement with the experimental data. Future research will be devoted to the simulation of interactions between multiple discs at various spacings.

Acknowledgements

References

[1] S. N. Butt, J. J. Timothy, and G. Meschke. Wave dispersion and propagation in state-based peridynamics. *Computational Mechanics*, Jul 2017.

[2] R. Gertsch, L. Gertsch, and J. Rostami. Disc cutting tests in colorado red granite: Implications for tbm performance prediction. *International Journal of rock mechanics and mining sciences*, 44(2):238–246, 2007.

[3] D. J. Littlewood. Roadmap for peridynamic software implementation. *SAND Report, Sandia National Laboratories, Albuquerque, NM and Livermore, CA*, 2015.

[4] J. Mitchell, S. Silling, and D. Littlewood. A position-aware linear solid constitutive model for peridynamics. *Journal of Mechanics of Materials and Structures*, 10(5):539–557, 2015.

[5] J. Rostami. *Development of a force estimation model for rock fragmentation with disc cutters through theoretical modeling and physical measurement of crushed zone pressure*. PhD thesis, Colorado School of Mines Golden, Colorado, USA, 1997.

[6] S. A. Silling and E. Askari. A meshfree method based on the peridynamic model of solid mechanics. *Computers & structures*, 83(17):1526–1535, 2005.

[7] S. A. Silling, M. Epton, O. Weckner, J. Xu, and E. Askari. Peridynamic states and constitutive modeling. *Journal of Elasticity*, 88(2):151–184, 2007.